MJSAT

Malaysian Journal of Science and Advanced Technology

journal homepage: https://mjsat.com.my/

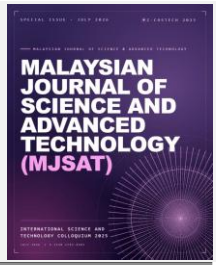

Comparative Study on the Corrosion Behaviour of Copper and Aluminium Electrodes in Seawater-Based Electrolysis systems

Nurin Fatini Afalatun[1], Sharifah Khadijah Alhabshi Syed Mokhdzar[1], Siti Aishah Mohamad Rizal[1], Nurul Izzatulhusna Khairul Anuar[1], Solhan Yahya[1], and Atikah Wan Nafi *[1]

[1]*Faculty of Applied Sciences, Universiti Teknologi MARA Perlis Branch, 02600 Arau, Perlis, Malaysia.*

KEYWORDS

Corrosion
Seawater
Electrochemical
Electrode

ARTICLE HISTORY

Received 22 November 2025
Available online 21 August 2026

ABSTRACT

Seawater; emerges as a promising source of renewable energy which generates electricity by utilizing the conductive properties of saline water. Seawater-lamp based energy device able to produce low-voltage power through electrochemical reactions between dissimilar metal electrodes. Nonetheless, the presence of complex ionic composition of seawater creates a harsh corrosive environment, hence reduces the electrode's longevity. Despite increasing interest in seawater battery, a research gap remains regarding the comparison of the role of chloride concentration on corrosion behaviour in natural seawater versus simplified salt solutions in active electrical circuits. Copper (Cu) and aluminium (Al) electrode pairs, which offer high potential difference and low material costs, were selected to address the lack of study on accelerated corrosion data for seawater battery. The aim of this study is to investigate the effects of varying chloride concentrations on electrode corrosion by comparing natural seawater with prepared sodium chloride (NaCl) solutions. Cu-Al electrode pairs were connected to a 2.5 V light bulb and utilized an impressed current. Corrosion rates were determined using the weight-loss method, while the surface characterization of electrodes deposition were further determined by optical microscopy, Scanning Electron Microscopy/Energy Dispersive X-ray (SEM/EDX), and Fourier Transform Infrared Spectroscopy (FTIR). The findings suggest that although seawater yielded higher electrical performance and brightest illumination, it also exhibited rapid deterioration, with Cu and Al exceeding corrosion rates of 40 mm/yr and 8 mm/yr, respectively. Overall, the study suggests that seawater, a viable energy source for the development of low-cost, off-grid lighting due to its abundant availability and low environmental effect.

1. INTRODUCTION

In light of increasing global energy demands and environmental concern, it is imperative to implement effective renewable energy technologies. Seawater has gained popularity around the world as an emerging renewable source for electricity generation due to its abundant availability, low environmental impact, simple system design, and potential for off-grid applications. A notable application is seawater lamp-based energy device, in which electrochemical reactions occur between the electrodes immersed in a seawater to generate electrical current, which subsequently powers a lamp [1 - 2].

The core component that enables a seawater lamp to function is salt, or sodium chloride (NaCl), one of the ionic compounds naturally found in seawater and the electrodes play a crucial role in facilitating the electrochemical reactions that generate electricity. In most widely available seawater lamps, a cell typically consists of magnesium anode paired with a carbon electrode for the cathode [3]. Although this configuration is effective, it has notable drawbacks such as magnesium's poor corrosion resistance and highly chemical reactive, leading to short device lifespans [4 - 5]. Therefore, these limitations highlight the need to explore alternative electrode materials.

*Corresponding author:
E-mail address: Atikah Wan Nafi < atikahnafi@uitm.edu.my >.
https://doi.org/10.56532/mjsat.v6iS1.804

Copper and aluminium emerge as promising alternatives owing to their lower cost than conventional materials and favourable electrochemical potential difference where the Cu-Al pair generates approximately 2.0 V compared to about 1.6 V for the Mg-C system [6-7]. Cu-Al electrodes practically be used in seawater battery as Al is known as lightweight and highly abundant material, while Cu with its exceptional electrical conductivity [8]. Moreover, Cu and Al form protective oxide layers which making them as good resistance to atmospheric corrosion [9 - 10]. However, their behaviour in high chloride concentration medium such as seawater, remains unknown.

Studies using Cu–Al electrodes have also demonstrated successful electricity generation with an output of 1.31 V ~ 2.55 V and from a Cu–Al seawater battery; confirming the feasibility of Cu–Al pairs as alternative energy sources [11 - 13]. However, the previous studies solely focus on electricity generation performance, with limited attention to electrode degradation. Few have compared corrosion behaviour in natural seawater versus controlled NaCl solutions at varying chloride concentrations.

The present work aimed to investigate the influence of prepared chloride concentration on corrosion behaviour of Cu and Al electrodes under active circuit compared with natural seawater. To gain deeper insight, the electrode surfaces were examined using optical microscopy, SEM/EDX, and FTIR spectroscopy. Additionally, this work assessed the relation between electrochemical performance and electrode longevity. Overall, understanding these corrosion mechanisms is essential for developing durable and cost-effective seawater energy systems with improved electrode protection strategies.

2. Materials and Method

2.1 Preparation of copper and aluminium electrodes

Electrodes with dimensions of 10 cm × 2 cm × 0.16 cm (length × width × thickness) were cut from copper and aluminium metal sheets, respectively. All electrode surfaces were abraded with 800-grit sandpaper were used to polish the oxide layer in order to ensure there are no contaminants adhering to the surface of the sample, then cleaned with acetone and distilled water and allowed to air dry in desiccator.

2.2 Preparation of saline solutions

Fresh seawater sample was collected from the seashore of Kuala Perlis, Perlis, Northern Peninsula of Malaysia. A known volume of the sample was filtered and boiled to evaporate the water. The remaining residue was dried in an oven until a complete crystalline product formed. The mass of the dried salt was recorded to estimate the salt content of the seawater. Based on the estimated salt concentration in the natural seawater, three NaCl (purchased from Sigma Aldrich) solutions of different molarities were prepared by dissolving specific amounts of NaCl powder in distilled water: 2.3 g (0.5 M), 4.0 g (0.88 M), and 6.0 g (1.25 M), respectively. These solutions served as a corrosive medium for the immersion tests to simulate a saline environment.

2.3 Immersion test

The tests were done following the setup by American Society of Testing and Materials (ASTM) protocols and shown in Figure 1 [14-15]. A pair of electrodes (Idea Toolroom) consisting of Al (anode) and Cu (cathode) was connected to a 2.5-volt light bulb and a power supply (PASCO scientific model SF-9584B) at 0.3V and 0.4A at ambient temperature. All immersion tests were performed for two-hour to ensure measurable corrosion while maintaining electrode integrity for surface characterization. The brightness of light bulb was observed as an indicator of electrical performance and circuit efficiency. The tests were duplicate and repeated using different concentration of NaCl solutions (0.5 M, 0.88 M, and 1.25 M). After immersion, the electrodes were removed from the solution and allowed to air dry in a desiccator before weighing.

2.4 Corrosion evaluation

Corrosion rate was determined through weight loss method. Each electrode was weighed prior to immersion to determine the initial mass and again after removal and drying to obtain the final mass. The weight loss, W_L was calculated using:

$$W_L = W_b - W_a \quad (1)$$

where W_b (g) was the weight of electrode before the immersion test, W_a (g) was the weight after the immersion test. The weight loss was used to calculate the corrosion rate, CR (mm/yr) using:

$$\text{Corrosion rate (mm/yr)} = (8.76\ W)/\rho At \quad (2)$$

where W was the weight loss (mg), ρ was the electrode density (g/cm^{-3}), A was the sample area (cm^2) and t was the immersion time in hours (h) [16]. All weight loss and corrosion rate measurements are reported as mean ± standard deviation (SD).

2.5 Surface characterization

The surface of the electrode samples was characterized by an optical microscope and Scanning Electron Microscopy (SEM) coupled with Energy Dispersive X-ray Spectroscopy (Phenom SEM Table Top system) at accelerating voltages of 15 kV, with magnifications ranging from 500x to 1500x. The corrosion products were further identified and confirmed by Perkin Elmer FTIR Spectrometer Frontier from 4000 to 400 cm^{-1}, with a high resolution of 2 cm^{-1}.

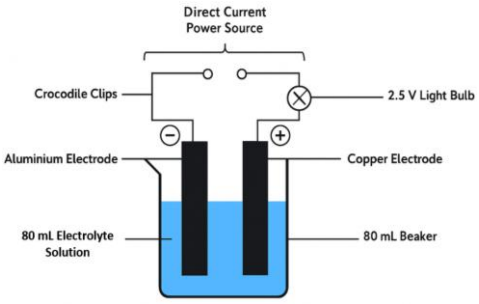

Fig. 1. Schematic showing an immersion test setup.

3. Results and Discussion

3.1 Electrical performance

From Figure 2, the light intensity at constant power supplied of 0.12W; varied across different electrolytes, with seawater producing the brightest illumination, followed by 1.25 M, 0.88 M, and 0.5 M NaCl solutions. This observation indicates that seawater provided superior electrical performance in powering the light bulb compared to pure NaCl

solutions. The observed brightness trend is consistent with established electrolyte behaviour [17]. While NaCl solutions provide primarily Na^+ and Cl^- ions as charge carriers, seawater contains a wider range of ions including SO_4^{2-}, Mg^{2+}, Ca^{2+}, and K^+ in addition to Na^+ and Cl^-, which produce higher current flow, ionic strength and lower the internal resistance of the cell [18-19].

3.2 Electrochemical mechanism

Copper is more noble than aluminium, with standard electrode potentials of $E°(Cu^{2+}/Cu) = +0.34$ V and $E°(Al^{3+}/Al) = -1.66$ V. This potential difference drives spontaneous electron flow from aluminium to copper through the external circuit, establishing aluminium as oxidation site (anode) and copper as the reduction site (cathode). In the external circuit, electrons flow from the aluminium electrode through the light bulb load to the copper electrode. Inside the electrolyte, electron was carried by the ions moving from copper to aluminium [20].

At the copper cathode, dissolved oxygen in the solution undergoes reduction:

$$O_2 + 2H_2O + 4e^- \rightarrow 4OH^- \quad (1)$$

This forms hydroxide ions (OH^-) in the area near the electrode. Although copper does not directly participate in the primary cell reaction, it serves as the electron acceptor and facilitates oxygen reduction [21]. The passage of electrons through copper enables the reduction of dissolved oxygen.

Naturally, upon exposure to air, aluminium spontaneously forms a thin, protective aluminium oxide layer (Al_2O_3) through rapid oxidation:

$$4Al + 3O_2 \rightarrow 2Al_2O_3 \quad (2)$$

This passivating layer, provides excellent corrosion resistance in neutral environments [22]. However, in chloride-containing electrolytes, chloride ions (Cl^-) destabilize the protective layer of aluminium.

At the aluminium anode, once the oxide barrier is compromised, oxidation occurs through reaction with the OH^- produced at the cathode:

$$Al + 3OH^- \rightarrow Al(OH)_3 + 3e^- \quad (3)$$

This reaction consumes aluminium metal and OH^- to produce solid aluminium hydroxide [$Al(OH)_3$]. The, chloride, Cl^- from the electrolyte migrates toward the aluminium anode to replace the OH^- consumed in this reaction and to facilitate passive film breakdown. The overall cell reaction, can be written stoichiometrically as:

$$4Al + 3O_2 + 6H_2O \rightarrow 4Al(OH)_3 \quad (4)$$

However, when copper is exposed to air, it readily oxidizes to form cuprous oxide (Cu_2O), which appears reddish, or cupric oxide (CuO), which appears black. In saline environments, copper still undergoes anodic dissolution through uniform corrosion mechanisms:

$$Cu \rightarrow Cu^+ + e^- \rightarrow Cu^{2+} + 2e^- \quad (5)$$

The copper ions (Cu^{2+}) subsequently react OH^- to form copper hydroxide [$Cu(OH)_2$] and basic copper chlorides such as atacamite [$Cu_2(OH)_3Cl$], which appear as greenish deposits on the copper surface. This behaviour aligned with electrochemical mechanism; local pH arising from large surface area, OH^- generation at the copper cathode, and formation of stable protective layer on copper to prevent aggressive action of chloride ions.

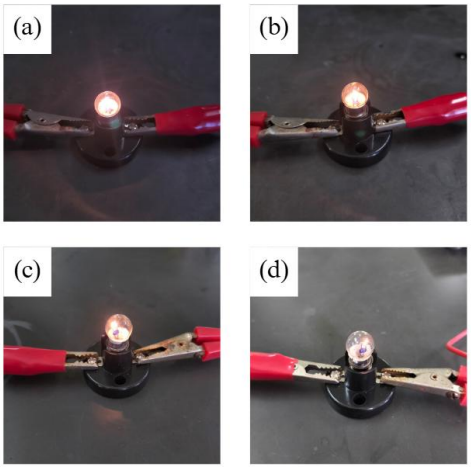

Fig. 2. Brightness of the lightbulb in a corrosion cell using different electrolytes: (a) Seawater; (b) 1.25 M NaCl; (c) 0.88 M NaCl; (d) 0.5 M NaCl.

3.3 Surface analysis

Figure 3 shown the microscopy images of aluminium and copper electrodes which both exhibited heterogeneous corrosion after immersion test.

The aluminium electrode from Figure 3(a) formed greyish-white surface deposits with rough, irregular patches across the surface. This morphology is characteristic of localized pitting corrosion [22]**.** Aluminium undergoes oxidation to form $Al(OH)_3$ at anodic sites (Equation 3). However, rather than forming uniformly, this corrosion localizes at vulnerable points where Cl^- have successfully penetrated and destabilized the protective Al_2O_3 layer. This localized pitting behaviour aligns with the previous findings; that in high-chloride electrolytes, the stability of the aluminium passive film is almost entirely compromised at specific nucleation sites. This pattern explains the low overall weight loss of aluminium compared to copper, as corrosion is concentrated rather than uniformly distributed across the entire surface [23-24].

In contrast, the copper electrode (Figure 3(b)) revealed greenish-white corrosion deposits; indicates metal dissolution experiences uniform corrosion on the entire surface [22]. This indicates the formation of $Cu(OH)_2$ and $Cu_2(OH)_3Cl$ [25]. The previous study explained that copper in natural seawater normally forms a porous, non-protective patina. However, while they reported that over time, copper patinas probably become protective, this study showed a continuous dissolution due to failure of formation of patina [26]. The uniform distribution of these oxidation products of aluminium, displayed that copper's corrosion mechanism involves active

dissolution without a significant protective barrier of Al_2O_3 in chloride environments.

Figure 4 shows the EDX analyses on corrosion products after immersion tests in 0.88 M seawater and 0.88 M NaCl. The deposits were composed predominantly of copper-based compounds; representing 93.92% and 90.77% of the metallic content in both solutions. In contrast, aluminium comprised only 6.08% and 9.23% of the detected metals. This demonstrates that copper dissolution was vigorous while aluminium was relatively less detectable, under the same tested parameters. This also explains the tendency of $Al(OH)_3$ layer to remain adhered to the surface and undissolved in the chloride environment, thus reducing their composition in corrosion products [27].

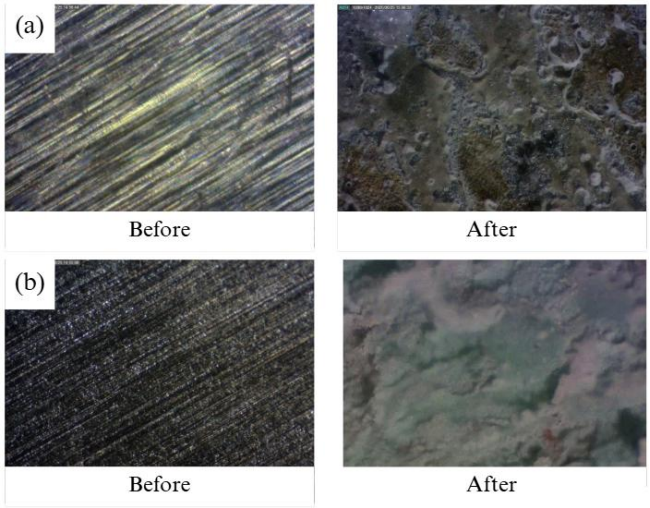

Fig. 3. Surface appearance of electrodes under optical microscope before and after immersion test: (a) Aluminium; (b) Copper.

The presence of hydroxide compounds on the electrode surface is shown on FTIR analysis (Figure 5). Strong and broad transmittance peaks displayed around 3323 cm^{-1} on all samples correspond to significant hydroxide formation on the electrode's deposited product [8]. The seawater-exposed samples showed the highest O–H peak intensities compared to other NaCl solutions. The natural seawater showed aggressive corrosion activity; probably due to the presence of various ionic species, including Cl^- initiating the dissolution of the passive film or pitting corrosion, while SO_4^{2-} serves as a secondary aggressive anion that penetrates the protective barrier. The dissolved oxygen accelerates electrochemical reactions through synergistic mechanisms, as it commonly acts as the primary cathodic reactant driving metal oxidation on the electrodes [16, 28]. The peak, at 1635 cm^{-1}, is related to H–O–H bending, suggesting that the precipitates contain bound water molecules, which are common in hydrated oxidation products [29]. Another peak at 1353 cm^{-1} represents the metal–oxygen bonding, possibly from Cu–O or Al–O structures. The peak around 1108 cm^{-1} is related to C–O stretching, which may originate from salt residues [30].

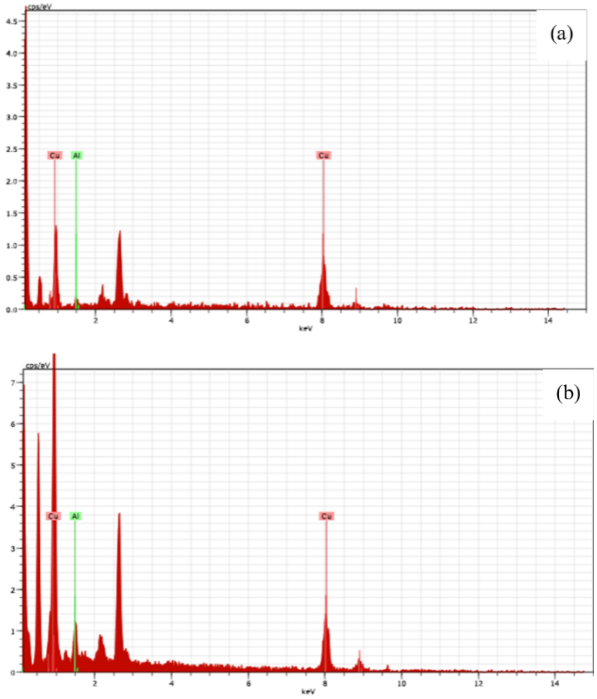

Fig. 4. EDX analyses of surface deposits: (a) seawater; (b) 0.88 M sodium chloride (NaCl)

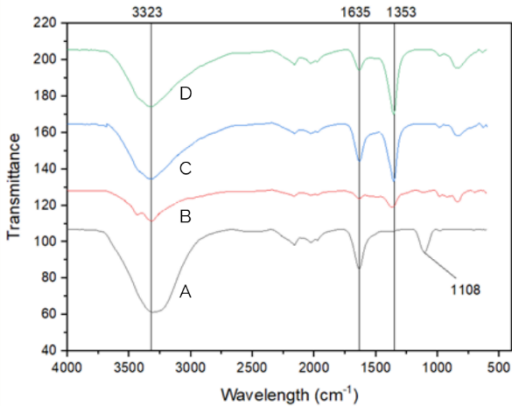

Fig. 5. FTIR spectra of surface deposits in: (A) seawater, (B) 0.5 M NaCl, (C) 0.88 M NaCl, and (D) 1.25 M NaCl.

3.4 Corrosion evaluation

Table 1 presents the weight loss (g) and corresponding corrosion rates (mm/yr) of copper and aluminium electrodes after immersion test in different electrolytes. Copper consistently exhibited higher weight loss and corrosion rates than aluminium under all test conditions. This is consistent with the findings; the dissolution of copper under electrolysis proceeds at a higher rate than the oxidation of aluminium [31 - 32].

The highest corrosion rate for copper and aluminium was demonstrated in seawater, while the lowest corrosion rates were recorded in 0.5 M NaCl for both electrodes. These results highlight that seawater is significantly more aggressive, despite

having a similar chloride concentration with 0.88 M NaCl solution. This confirms that the corrosion reaction in seawater does not solely depend on chloride concentration. Which means, the additional presence of SO_4^{2-}, Mg^{2+}, and Ca^{2+} facilitates pitting corrosion in seawater by increasing the electrolyte's total ionic strength and conductivity, hence breakdown the passive Al_2O_3 protection layer [11].

Table 1 Weight loss and corrosion rate of Aluminium and Copper electrodes after immersion test.

Solution	E	Sample	W_L (g)	W_L (Mean ± SD)	CR (mm/yr)	CR (Mean ± SD)
Seawater	Cu	A1	0.8373	0.8565 ± 0.0271	40.39	41.6 ± 1.71
		A2	0.8756		42.81	
	Al	A1	0.0532	0.0511 ± 0.003	8.63	8.29 ± 0.49
		A2	0.0489		7.94	
0.5 M NaCl	Cu	B1	0.5890	0.6053 ± 0.023	28.79	29.59 ± 1.12
		B2	0.6215		30.38	
	Al	B1	0.0350	0.0364 ± 0.002	5.68	5.91 ± 0.32
		B2	0.0378		6.13	
0.88 M NaCl	Cu	C1	0.6500	0.6673 ± 0.0244	31.77	32.62 ± 1.19
		C2	0.6845		33.46	
	Al	C1	0.0410	0.0423 ± 0.0018	6.65	6.87 ± 0.30
		C2	0.0436		7.08	
1.25 M NaCl	Cu	D1	0.8434	0.8163 ± 0.0383	41.23	39.91 ± 1.87
		D2	0.7892		38.58	
	Al	D1	0.0448	0.046 ± 0.0016	7.27	7.46 ± 0.26
		D2	0.0471		7.64	

In contrast, a clear trend was shown in the NaCl solutions; increasing the concentration up to 1.25 M (~7.3% NaCl) for both metal electrodes will increase the corrosion rate. This behaviour can be explained by the role of chloride ions in actively accelerating passivating layer breakdown of Al_2O_3. In addition, the increased ionic strength of the electrolyte allows greater galvanic current flow between the Cu-Al couple that may override oxygen-limitation effects [33 - 35]. However, one of the previous findings reported that in high saline environments (within 3–5% NaCl), the study successfully lowered the solubility of dissolved oxygen, thus reducing the corrosion rate [16].

Based on the presented corrosion rates in Table 1, the operational lifespan of the Cu-Al electrodes can be estimated to determine the practicality to use in the seawater lamp or device. For electrodes, the copper cathode with a thickness of 1.6 mm seems to be the primary limiting factor for device longevity. In seawater, where the corrosion rate of copper reaches 41.60 mm/yr; the complete deterioration would occur in approximately 14 days of continuous operation. Even under the 0.5 M NaCl, the device lifespan of the copper electrode only extends to approximately 20 days.

These findings reveal a fundamental relation between electrochemical performance and electrode durability that must be addressed in the design of seawater-based energy devices. Utilizing seawater potentially generates electricity but their performance was hindered by rapid device failure. This study also suggests the importance of future study on the implementation of advanced corrosion protection techniques such as protective coatings or organic inhibitors to provide a sustainable solution for long-term applications of energy devices from the renewable source of seawater.

4. CONCLUSION

These results highlight the performance and durability of electrodes in seawater and NaCl solutions. Specifically, the study proved that while seawater provides the brightest illumination, it simultaneously accelerates the uniform corrosion of the copper cathode to 41.60 ± 1.71 mm/yr. This rate is significantly higher than that of equivalent NaCl solutions. Unlike immersion studies where corrosion rates typically peak at 3.5% NaCl, the active electrical load in this system overrides oxygen-solubility limitations, leading to a continuous increase in corrosion rates. Surface analysis elucidated the degradation mechanisms of the electrode. FTIR spectra indicated the presence of hydroxyl groups, aggressive ionic species, and metal–oxygen bonds, highlighting ongoing corrosion processes. Complementary EDX analysis confirmed the formation of corrosion products with specified metal and oxide compositions. Observed changes in oxide color provide evidence supporting the proposed mechanisms of electrode degradation.

Despite these insights, the study relied on qualitative light intensity observations rather than electrolytic conductivity measurements. While the light intensity provided a clear qualitative indicator of electrical performance, the lack of precise conductivity values (mS/cm) means that the exact relationship between ionic strength and internal cell resistance was not quantitatively mapped. Although, the observed trends indicate clear differences between electrolyte conditions, formal statistical hypothesis testing such as ANOVA was not undertaken due to the limited sample size. Future work should incorporate larger sample sizes to enable statistical validation of the differences in corrosion rates. Although potential uncertainties were minimized in this study to ensure reproducibility and precision, future work should rigorously consider factors such as immersion technique, sample weighing, solution pH, and electrode surface uniformity to achieve accuracy.

These findings are significant for the development of low-cost, off-grid lighting. The results indicate that unprotected Cu-Al couples are unsuitable for long-term sustainable use, regardless of the electrolyte used. Future research should focus on exploring the integration of protective coatings that allow ionic transport while slowing the dissolution of the copper cathode.

ACKNOWLEDGEMENT

The authors thank Dr Peter McIntyre from UNSW for his generous and substantial contributions in editing this work.

REFERENCES

[1] J. Chen, W. Xu, X. Wang, S. Yang, and C. Xiong, "Progress and applications of seawater-activated batteries," *Sustainability*, vol. 15, no. 2, pp. 1635, Jan. 2023, doi: https://doi.org/10.3390/su15021635.

[2] S. Li and X. Tian, "Progress of seawater batteries: from mechanisms, materials to applications," *Journal of Power Sources*, vol. 617, pp. 235161–235161, Aug. 2024, doi: https://doi.org/10.1016/j.jpowsour.2024.235161.

[3] N. A. Bani et al., "Feasibility study of a low cost saltwater lamp for rural area," *International Journal of Integrated Engineering,* vol. 10, no. 7, Nov. 2018, doi: https://doi.org/10.30880/ijie.2018.10.07.016.

[4] A. Azizi Amirabad, M. Johari, R. Parichehr, R. Mehdinavaz Aghdam, C. Dehghanian, and S. R. Allahkaram, "Improving corrosion, antibacterial and biocompatibility properties of MAO-coated AZ31 magnesium alloy by Cu(II)-chitosan/PVA nanofibers post-treatment," *Ceramics International,* vol. 49, no. 11, pp. 17371–17382, Jun. 2023, doi: https://doi.org/10.1016/j.ceramint.2023.02.106.

[5] S. Pommiers, J. Frayret, A. Castetbon, and M. Potin-Gautier, "Alternative conversion coatings to chromate for the protection of magnesium alloys," *Corrosion Science*, vol. 84, pp. 135–146, Jul. 2014, doi: https://doi.org/10.1016/j.corsci.2014.03.021

[6] B. Craig, T. Schoetz, A. Cruden, and C. P. de Leon, "Review of current progress in non-aqueous aluminium batteries," *Renewable and Sustainable Energy Reviews*, vol. 133, pp. 110100, Nov. 2020, doi: https://doi.org/10.1016/j.rser.2020.110100

[7] B. Rani, J. K. Yadav, P. Saini, A. P. Pandey, and A. Dixit, "Aluminium–air batteries: Current advances and promises with future directions," *RSC Advances*, vol. 14, no. 25, pp. 17628-17663, June 2024, doi: https://doi.org/10.1039/D4RA02219J

[8] S. Lamghafri et al., "Promising corrosion resistance of mild steel, copper, and aluminum in hydrochloric acid solution using an environmentally friendly corrosion inhibitor," *Journal of Industrial and Engineering Chemistry,* vol. 146, pp. 332-348, Nov. 2024, doi: https://doi.org/10.1016/j.jiec.2024.11.016.

[9] S. B. Adeloju and H. C. Hughes, "The corrosion of copper pipes in high chloride-low carbonate mains water," *Corrosion Science*, vol. 26, no. 10, pp. 851–870, Jan. 1986, doi: https://doi.org/10.1016/0010938X(86)90068-5

[10] T. Suter, E. M. Moser, and H. Böhni, "The characterization of the tarnishing of Cu-15Ni-8Sn and Cu-5Al-5Sn alloys," *Corrosion Science*, vol. 34, no. 7, pp. 1111–1122, Apr. 2003, doi: https://doi.org/10.1016/0010-938X(93)90292-O.

[11] A. Susanto et al., "Performance of Zn-Cu and Al-Cu Electrodes in Seawater Battery at Different Distance and Surface Area." *International Journal of Renewable Energy Research*, vol.7, no. 1, 2017, doi: https://doi.org/10.20508/ijrer.v7i1.5506.g7018.

[12] M. R. Kadir et al., "Seawater Lamp: Utilization of Seawater as an Alternative Energy Source to Generate Electricity," *Indones. Rev. Phys.,* vol. 6, no. 1, pp. 17–23, 2023, doi: https://doi.org/10.12928/irip.v6i1.7070.

[13] D. Anwar, J. N. T. Papia, H. Purnomo, and P. D. Darmawan, "Design and Performance Testing of Seawater Batteries as Renewable Energy for Marine Boat Lights," *International Journal of Recent Technology and Applied Science*, vol. 7, no. 1, pp. 26-32, March 2025, doi: https://doi.org/10.36079/lamintang.ijortas-0701.773

[14] *ASTM, 2003 Annual book of ASTM standards. Designation G1- 90: Standard practice for preparing, cleaning, and evaluation corrosion test specimens. Philadelphia, PA: ASTM, 2003.* url: https://store.astm.org/g0001-03.html

[15] *ASTM,* 1999 *Annual* book of ASTM standards. Designation G31- 72: Standard practice for laboratory immersion corrosion testing and materials preparing. Philadelphia, PA: ASTM, 1999. url: https://store.astm.org/g0031-72r04.html

[16] F. Brownlie, T. Hodgkiess, A. Pearson, and A. Galloway, "Electrochemical evaluation of the effect of different NaCl concentrations on low alloy- and stainless steels under corrosion and erosion-corrosion conditions," *Corrosion and Materials Degradation*, vol. 3, no. 1, pp. 101–126, Feb. 2022, doi: https://doi.org/10.3390/cmd3010006

[17] J. Wang, G. I. Waterhouse, N. Liu, J. Kennedy, W. Gao, and S. Wei, "Primary Magnesium-air Batteries Performance Comparison: 3.5 wt.% NaCl vs Natural Seawater as the Electrolyte," *Electrochimica Acta*, pp. 147869, 2025, doi: https://doi.org/10.1016/j.electacta.2025.147869

[18] K. El Kadi, S. Murad, and I. Janajreh, "Electric field-assisted freeze desalination: Effects on ion transport, water structure, and ice growth rates," *Energy Nexus*, pp. 100585, Dec. 2025, doi: https://doi.org/10.1016/j.nexus.2025.100585

[19] E. Yang, M. J. Choi, K. Y. Kim, K. J. Chae, and I. S. Kim, "Effect of initial salt concentrations on cell performance and distribution of internal resistance in microbial desalination cells," *Environmental Technology*, vol. 36, no. 7, pp. 852–860, Sep. 2014, doi: https://doi.org/10.1080/09593330.2014.964333.

[20] N. A. Rahman, C. J. Jol, A. A. Linus, B. H. M. Jan, A. Parabi, C. K. Ming, and D. F. A. A. A. Hamid, "Corrosion Resistance and Electrochemical Adaptation of Aluminium in Brackish Peat Water Sources Under Seawater Intrusion in the Rural Tropical Peatlands of Borneo," *Sustainable Chemistry for Climate Action*, pp. 100074, June 2025, doi: https://doi.org/10.1016/j.scca.2025.100074

[21] L. A. R. Cañete, "A Comparison of the Performance of Saltwater Electrolytic Cell Battery with Zinc-Copper and Aluminium-Copper Electrodes," *International Research Journal of Pure and Applied Chemistry*, vol. 25, no. 1, pp. 1-21, Jan. 2024, doi: https://doi.org/10.9734/irjpac/2024/v25i1841

[22] A. Wan Nafi, A. Afifi, N. A. Zainal Abidin, N. H. Abdul Aziz, and K. Kalantari, "Effect of the Poly L-lactic Acid Coating on the Corrosion of Magnesium in Hank's Solution," *Sains Malaysiana*, vol. 47, no. 1, pp. 169–179, Jan. 2018, doi: https://doi.org/10.17576/jsm-2018-4701-20.

[23] Masrufaiyah, et al., "Performance of Seawater Activated Battery as Alternative Energy Resources." *IPTEK Journal of Engineering*, vol. 3, no. 1, pp. 11, May. 2017, doi: https://doi.org/10.12962/joe.v3i1.2266.

[24] Z. Smialowska, "Pitting Corrosion of Aluminium," *Corrosion Science*, vol. 41, no. 9, pp. 1743–1767, Aug. 1999, doi: https://doi.org/10.1016/S0010-938X(99)00012-8.

[25] A. Fateh et al., "Review of Corrosive Environments for Copper and Its Corrosion Inhibitors." *Arabian Journal of Chemistry*, vol. 13, no. 1, pp. 481–544, Jan. 2020, doi: https://doi.org/10.1016/j.arabjc.2017.05.021.

[26] K. P. Fitzgerald et al., "The Chemistry of Copper Patination." *Corrosion Science*, vol. 40, no. 12, pp. 2029–2050, Dec. 1998, doi: https://doi.org/10.1016/S0010-938X(98)00093-6.

[27] M. Magnan, S. Zanna, A. Seyeux, F. Wiame, and J. Światowska, "Corrosion evolution of aluminium-copper and aluminium-copper-lithium alloys in chloride solution," *Applied Surface Science*, pp. 163922, Jun. 2025, doi: https://doi.org/10.1016/j.apsusc.2025.163922.

[28] N. A. Rahman, C. J. Jol, A. A. Linus, S. N. L. Taib, A. Parabi, C. K. Ming, and D. F. A. A. Hamid, "Unveiling challenges of aluminium electrode fouling and passivation in electrocoagulation treatment system for sustainable water management of coastal Borneo peatlands: A focused review," *Environmental Research*, pp. 121005, Apr. 2025, doi: https://doi.org/10.1016/j.envres.2025.121005

[29] T. D. Kerf, G. Pipintakos, Z. Zahiri, S. Vanlanduit, and P. Scheunders, "Identification of corrosion minerals using shortwave infrared hyperspectral imaging," *Sensors*, vol. 22, no. 1, p. 407, Jan. 2022, doi: https://doi.org/10.3390/s22010407.

[30] J. P. Labbé, J. Lédion, and F. Hui, "Infrared spectrometry for solid phase analysis: Corrosion rusts," *Corrosion Science*, vol. 50, no. 5, pp. 1228–1234, May 2008, doi: https://doi.org/10.1016/j.corsci.2007.08.023.

[31] M.V. Yarmolenko and S.O. Mogilei. "Copper and Aluminium Electrochemical Corrosion Investigation during Electrolysis and Heating from 20°C to 180°C." Physics and Chemistry of Solid State, vol. 24, no. 4, pp. 765–773, Dec. 2023, doi: https://doi.org/10.15330/pcss.24.4.765-773.

[32] L. Reidy, C. Wang, and C. L. Hussey, "Anodic dissolution of copper in the acidic and basic aluminum chloride 1-ethyl-3-methylimidazolium chloride ionic liquid," *Journal of The Electrochemical Society*, vol. 168, no. 4, pp. 046503, Apr. 2021. doi: https://doi.org/10.1149/1945-7111/abebfa

[33] C. Blanc, N. Pébère, B. Tribollet, and V. Vivier, "Galvanic coupling between copper and aluminium in a thin-layer cell," *Corrosion Science*, vol. 52, no. 3, pp. 991–995, 2010, doi: https://doi.org/10.1016/j.corsci.2009.11.023

[34] F. C. Walsh, B. D. Barker, K. R. Stokes, and G. Kear, "Corrosion of Copper, Cupronickel, Nickel Aluminium Bronze and Super-Duplex Stainless Steel Rotating Cylinder Electrodes in Seawater under Turbulent Flow Conditions," *Journal of The Electrochemical Society*, vol. 171, no. 10, pp. 101503, Oct. 2024, doi: https://doi.org/10.1149/1945-7111/ad81b5

[35] J. H. Huh, S. H. Kim, J. H. Chu, S. Y. Kim, J. H. Kim, and S. Y. Kwon, "Enhancement of seawater corrosion resistance in copper using acetone-derived graphene coating," *Nanoscale*, vol. 6, no. 8, pp. 4379-4386, March 2014, doi: https://doi.org/10.1039/c3nr05997a